Polymer Chemistry

PAPER

View Article Online
View Journal | View Issue

Published on 20 May 2016. Downloaded by Synchrotron Radiation Library on 11/09/2017 09:39:33.

Cite this: *Polym. Chem.*, 2016, **7**, 4046

Approaching high charge carrier mobility by alkylating both donor and acceptor units at the optimized position in conjugated polymers†

Dong Gao,‡[a,b] Kui Tian,‡[a,b] Weifeng Zhang,‡[a] Jianyao Huang,[a] Zhihui Chen,[a,b] Zupan Mao[a,b] and Gui Yu*[a,b]

Received 16th March 2016,
Accepted 15th May 2016

DOI: 10.1039/c6py00469e

www.rsc.org/polymers

Flexible side chains have been the central issue in the design of solution-processable polymer semiconducting materials. On identical conjugated backbones, great differences can be made with different side chain densities and substitution positions. Generally, for donor–acceptor (D–A) copolymers, increasing the side chain density could readily improve the solubility of the polymers. However, it also results in backbone distortion and weaker interchain interactions, thus hindering charge transport, which limits the application of highly soluble D–A polymers. Herein, we synthesized two polymers of PD-*n*-DTTE-7 with both the moieties alkylated. Substituting side chains to DTTE units improved the solubility of the corresponding polymers. Induced by the promoted solubility, high purity of the high molecular weight component was obtained and uniform films were formed with these high molecular weight polymers. In addition, by carefully selecting the conjugation system and substitution positions, ordered packing and backbone coplanarity were also achieved, which facilitate interchain and intrachain charge transport. Through a simple spin coating technique, the polymers, PD-*n*-DTTE-7s, present the highest hole mobility of 9.54 $cm^2\ V^{-1}\ s^{-1}$ with high average mobilities of over 5 $cm^2\ V^{-1}\ s^{-1}$, which are among the highest values for polymer-based field-effect transistors.

Introduction

Polymer semiconductors have been widely studied due to their potential applications in low cost and large area thin film transistors.[1] During the last few years, remarkable efforts have been made to improve the field-effect properties and impressively high mobilities of exceeding 10 $cm^2\ V^{-1}\ s^{-1}$ have been achieved.[2] Among the semiconducting materials for high-performance organic field-effect transistors (OFETs), diketopyrrolopyrrole (DPP)-based donor–acceptor (D–A) copolymers have attracted much more attention with their remarkably high mobilities owing to the aggregation properties of DPP moieties.[3]

In the design of polymer semiconductors for OFETs, the selection and substitution position of alkyl chains has been an interesting and complex scientific issue.[2f,4] The structure and density of aliphatic substituents exert great influences on improving the thin film microstructure and morphology, thus affecting the charge transport properties of related polymers.[5] Increasing the molecular weight is an effective way for enhancing the FET performance.[6] However, solubility problems can also result from a very high molecular weight, which disrupts the thin film uniformity.[7] The increasing alkyl side chain density could afford better solubility, which is essential for solution processing. However, the side chain interdigitation is somewhat hindered.[5c,8] Generally, the alkyl side chains are substituted either on donor or on acceptor moieties. Some studies reported decreased charge carrier mobilities for the D–A polymers with alkyl chains substituted on each unit compared with those on either donors or acceptors, although the solubility of polymers was improved.[9] Theoretical studies implied that unsuitable substitution positions on the polymer backbone could increase the dihedral angle and torsional disorder along the π-conjugated backbone, thus leading to serious π-conjugated skeleton distortion. The large distortion of the polymer backbone could result in a decreased effective conjugation length, which exerts negative influences on intrachain charge transport. In addition, when the polymers are stacked together, steric hindrance may exist between the neighbouring polymer chains because of the side chain repulsion. Therefore, the interchain charge transport is limited. On the basis of the aforementioned understanding, the concept of "molecular docking" was proposed by Pei *et al.*, part of which means designing a small unit without alkyl side chains with

[a]*Beijing National Laboratory for Molecular Sciences, Institute of Chemistry, Chinese Academy of Sciences, Beijing 100190, P. R. China. E-mail: yugui@iccas.ac.cn*
[b]*University of Chinese Academy of Sciences, Beijing 100049, P. R. China*
†Electronic supplementary information (ESI) available. See DOI: 10.1039/c6py00469e
‡These authors contributed equally to this work.

This journal is © The Royal Society of Chemistry 2016

Published on 20 May 2016. Downloaded by Synchrotron Radiation Library on 11/09/2017 09:39:33.

the aim of docking into a large aromatic core. The design method can reduce the steric hindrance generated where polymers are stacked with each other, which improves the π–π interaction between the neighbouring polymer chains.[9e] This strategy is applicable to many high-performance D–A type copolymers, especially DPP-based polymers. For the large unit with sufficiently wide space for "molecular docking", however, it becomes acceptable to introduce alkyl side chains on both the donor and acceptor units as the steric hindrance originating from the alkyl side chains could be partially avoided. When longer π-conjugated units with alkyl chain substituents are introduced into the polymer backbone, the cavity between the side chains of donor and acceptor units will be larger for the alkylated units of other polymers to "dock". Moreover, by selecting suitable substitution sites, backbone distortion arising from the steric hindrance between the side chains and the atoms or groups on the backbone could also be minimized.

Herein, we reported two new soluble alternating alkylated di(thienothienyl)ethylene (DTTE) based copolymers PD-*n*-DTTE-7 with different branched side chains on DPP moieties. Extending the π-conjugation of building blocks has been an effective effort to improve the device performance.[10] Compared with thiophene units, the centrosymmetric thieno[3,2-*b*]thiophene units show a similar planarity and a higher conjugation degree. Introducing thieno[3,2-*b*]thiophene into the polymer main chains has been theorized to increase the coplanarity and rigidity of the polymer backbone, offering better π-orbital overlap, thus facilitating the intra- and intermolecular charge transport.[11] DTTE-based polymers have been reported to exhibit a hole mobility of 3.13 $cm^2 V^{-1} s^{-1}$, suggesting DTTE units to be a promising building block for high-performance polymer semiconductors.[12] Alkyl chains were introduced at the middle of the DTTE moiety to maximize the cavity between the side chains. In addition, to maintain the coplanarity of the backbone for PD-*n*-DTTE-7, heptyl groups are substituted at the positions adjacent to the vinylene linkage. FETs fabricated from PD-*n*-DTTE-7 exhibit a hole mobility of up to 9.54 $cm^2 V^{-1} s^{-1}$, to our knowledge, which is one of the highest values for DPP-based polymer FETs.

Experimental section

General procedures and requirements

The catalysts, chemicals, and solvents used were purchased from commercial sources, and were used without further purification. Tetrahydrofuran (THF) was freshly distilled over sodium and benzophenone. The DPP monomers were synthesized according to the previous literature,[1a] and 3-heptylthieno[3,2-*b*]thiophene (compound **1**) was synthesized by following the literature methods.[13]

Measurements and characterization

^{1}H-NMR and ^{13}C-NMR spectra were recorded on a Bruker Avance 300 MHz and 400 MHz spectrometer. High-resolution Electron-impact mass spectra (HREI-MS) were collected on a Bruker APEX II mass spectrometer. High-resolution MALDI-TOF (HRTOF-MS) was performed on a Bruker 9.4T Solarix mass spectrometer. Gel-permeation chromatography (GPC) was performed on an Agilent PL-GPC 220 using polystyrene as a standard and 1,2,4-trichlorobenzene stabilized with 0.0125% BHT as an eluent. UV–vis absorption spectra were obtained in the polymer solutions and polymer thin films using a PE Lambda 25 spectrometer. Cyclic voltammetry (CV) experiments were conducted on an electrochemistry workstation (CHI660c, Chenhua, Shanghai) using a three-electrode cell. An Ag/AgCl (Ag in 0.01 mol L^{-1} KCl) electrode was used as a reference electrode and a platinum wire was used as a counter electrode. A platinum stick electrode coated with a thin film layer of polymers was used as a working electrode. An anhydrous and N_2-saturated solution of 0.1 M tetrabutylammonium hexylfluorophosphate in acetonitrile was employed as an electrolyte. Thermogravimetric analysis (TGA) was performed on a Perkin-Elmer TGA-7 with a heating rate of 10 °C min^{-1} under an inert atmosphere. The films of the polymers were imaged in air using a Digital Instruments Nanoscope V atomic force microscope operated in tapping mode (Table 1).

2-Bromo-3-heptylthieno[3,2-*b*]thiophene (2). *N*-Bromosuccinimide (1.11 g, 6.25 mmol) was added in portions to a solution of **1** (1.48 g, 6.20 mmol) in a mixture of chloroform and dimethylformamide at 0 °C. After stirring the solution for 2 h at ambient temperature, water was added and the aqueous layer was extracted with dichloromethane. The organic layers were washed with brine and dried over anhydrous Na_2SO_4. The solvent was removed in a vacuum, and the residue was purified by chromatography on silica gel eluting with hexane to give **2** (1.53 g, 78%) as a colourless oil. ^{1}H-NMR (400 MHz, CD_2Cl_2): δ (ppm) 7.48 (d, J = 8 Hz, 1H), 7.24 (d, J = 8 Hz, 1H), 2.81 (t, J = 7.5 Hz, 2H), 1.75 (tt, J = 8, 8 Hz, 2H), 1.29–1.34 (br, 8H), 0.94 (t, J = 16 Hz, 3H). ^{13}C-NMR (101 MHz, CD_2Cl_2): δ 138.35, 136.61, 134.32, 125.93, 119.54, 109.92, 31.85, 29.20, 29.09, 28.99, 27.87, 22.62, 13.82. HR-MS (EI) m/z: Anal. Calcd for

Table 1 Properties of the polymers PD-8-DTTE-7 and PD-10-DTTE-7

Polymer	M_n (kDa)	PDI	Solubility[a] (mg mL^{-1})	T_d [b] (°C)	λ_{max} (solution) (nm)	λ_{max} (film) (nm)	Band gap[c] (eV)	HOMO (eV)
PD-8-DTTE-7	74	2.75	4.22	352	790	792	1.26	−5.32
PD-10-DTTE-7	182	2.91	6.45	320	790	796	1.25	−5.33

[a] The solubility was measured in the DCB solvent. [b] Temperature at 5% weight loss under nitrogen. [c] Estimated from the onset wavelength of the absorption in the films.

Published on 20 May 2016. Downloaded by Synchrotron Radiation Library on 11/09/2017 09:39:33.

$C_{13}H_{17}BrS_2$: 315.9955 (^{79}Br), 317.9935 (^{81}Br). Found: 315.9958 (^{79}Br), 317.9953 (^{81}Br).

3-Heptylthieno[3,2-*b*]thiophene-2-carbaldehyde (3). To a 100 mL round-bottomed flask, **2** (7.1 g, 22.3 mmol) and 50 mL of dry THF were added under a N_2 atmosphere, then the mixture was cooled down to −78 °C and *n*-butyllithium (8.95 mL, 2.5 M in hexane) was added dropwise. After stirring at −78 °C for 0.5 h, 1-formylpiperidine (3.3 g, 28.99 mmol) was added to the solution immediately. The mixture was then warmed to room temperature and stirred overnight. The solution was extracted with ethyl acetate and dried with anhydrous Na_2SO_4. **3** (4.93 g, 83%) was purified by silica gel chromatography with an eluent of 15% ethyl acetate/hexane to afford a yellow oil. ^{1}H-NMR (400 MHz, CD_2Cl_2): δ (ppm) 10.11 (s, 1H), 7.66 (d, J = 5.4 Hz, 1H), 7.31 (d, J = 5.4 Hz, 1H), 2.77 (t, J = 7.5 Hz, 2H), 1.76 (t, J = 5.4, 8 Hz, 2H), 1.29–1.34 (br, 8H), 0.88 (t, J = 7.8 Hz, 3H). ^{13}C-NMR (75 MHz, CD_2Cl_2): δ 145.08, 144.36, 141.10, 139.93, 132.92, 120.53, 36.33, 31.56, 31.20, 30.99, 29.67, 26.73, 15.92. HR-MS (EI) *m*/*z*: Anal. Calcd for $C_{14}H_{18}OS_2$: 266.0799. Found: 266.0801.

(*E*)-1,2-Bis(3-heptylthieno[3,2-*b*]thiophen-2-yl)ethene (4). $TiCl_4$ (19 mL, 1 M in toluene) was added slowly using a syringe to a stirred suspension of zinc (2.35 g, 36 mmol) powder in anhydrous tetrahydrofuran at 0 °C under a N_2 atmosphere. The mixture was heated at 70 °C for 6 h. The suspension was cooled to room temperature and **3** (2.4 g, 9 mmol) was added at once. The resulting mixture was then heated and refluxed overnight. After the reaction, saturated sodium carbonate was added and the mixture was passed through a Celite pad, which was washed with dichloromethane. The filtrate was extracted with dichloromethane and purified by silica gel chromatography with hexane to yield **4** (1.35 g, 60%) as a bright yellow solid. ^{1}H-NMR (300 MHz, $CDCl_3$): δ (ppm) 7.31 (d, J = 5.1 Hz, 2H), 7.14 (d, J = 5.1 Hz, 2H), 7.01 (s, 2H), 2.75 (t, J = 7.5 Hz, 4H), 1.75 (tt, J = 7.5, 7.2 Hz, 4H), 1.21–1.29 (br, 16H), 0.79 (t, J = 6.6 Hz, 6H). ^{13}C NMR (75 MHz, CD_2Cl_2): δ 141.48, 138.33, 135.76, 133.02, 127.07, 119.89, 119.82, 31.78, 29.39, 29.29, 29.07, 28.17, 22.67, 13.85. HR-MS (TOF) *m*/*z*: Anal. Calcd for $C_{28}H_{36}S_4$: 500.169437. Found: 500.169582.

(*E*)-1,2-Bis(5-(trimethylstannyl)-3-heptylthieno[3,2-*b*]thiophen-2-yl)ethene (5). *n*-BuLi (1.67 mL, 2.5 M in hexane) was added dropwise to a solution of **4** (1 g, 1.99 mmol) in anhydrous THF under −78 °C. The suspension was stirred for 1 h, after which a 1.0 M solution of trimethyltin chloride (8.2 mL) in THF was added at once at −78 °C, and then the mixture was stirred for another 3 h at −50 °C. The mixture was quenched with water, extracted with ether, then washed with brine, and the combined organic extracts were dried over anhydrous Na_2SO_4 and concentrated. The crude solid obtained was purified by recrystallization from dichloromethane and methanol to yield the title compound as an orange solid (1.16 g, 70%). ^{1}H-NMR (300 MHz, $CDCl_3$): δ (ppm) 7.16 (s, 2H), 6.99 (s, 2H), 2.74 (t, J = 7.5 Hz, 4H), 1.65 (tt, J = 7.2, 7.5 Hz, 4H), 1.21–1.29 (br, 16H), 0.80 (t, J = 6.9 Hz, 6H), 0.33 (s, 18H). ^{13}C NMR (75 MHz, CD_2Cl_2): δ 146.98, 141.62, 138.33, 137.54, 132.54, 126.94, 119.83, 31.80, 29.41, 29.32, 29.08, 28.28, 22.69, 13.87, −8.53. HR-MS (TOF) *m*/*z*: Anal. Calcd for $C_{34}H_{52}S_4Sn_2$: 826.099461. Found: 826.099745.

Synthesis of PD-8-DTTE-7. In a Schlenk flask, (*E*)-1,2-bis(5-(trimethylstannyl)-3-heptylthieno[3,2-*b*]thiophen-2-yl)ethane (**5**, 165.29 mg, 0.2 mmol), 3,6-bis-(5-bromothiophen-2-yl)-*N*,*N*-bis(2-octyldodecyl)-1,4-dioxo-pyrrolo[3,4-*c*]pyrrole (**6**, 203.84 mg, 0.2 mmol), tris(dibenzylideneacetone)dipalladium(0) (4.5 mg) and tri(*o*-tolyl)phosphine (12.3 mg) were dissolved in dry toluene (10 mL). The solution was charged with nitrogen through a freeze pump thaw cycle three times, and then the mixture was stirred at 110 °C for 1 h under a nitrogen atmosphere. The polymer was precipitated in a mixture of methanol and 1 M aqueous HCl solution (with a ratio of 10 : 1) after cooling down to room temperature. The crude polymer was collected by filtration and then purified by Soxhlet extraction with methanol, acetone, hexane, chloroform, and chlorobenzene successively. The evaporation of chlorobenzene fractions afforded a dark solid. GPC: M_n = 74 kDa, PDI = 2.75; ^{1}H NMR (300 MHz, $C_2D_2Cl_4$, 110 °C) δ (ppm): 7.93 (br, 2H), 7.30 (br, 4H), 6.91 (br, 2H), 4.27 (br, 4H), 0.80–1.90 (m, 108H).

Synthesis of PD-10-DTTE-7. The synthesis of PD-10-DTTE-7 follows the same operating process as that of PD-8-DTTE-7. GPC: M_n = 182 kDa, PDI = 2.91; ^{1}H NMR (300 MHz, $C_2D_2Cl_4$, 110 °C) δ (ppm): 7.88 (br, 2H), 7.30 (br, 4H), 6.88 (br, 2H), 4.26 (br, 4H), 0.81–1.32 (m, 124H).

Device fabrication and characterization

Polymer-based FETs were fabricated on highly-doped silicon wafer with a 300 nm SiO_2 insulator with source–drain gold electrodes formed by photolithography. The substrates were subjected to cleaning by ultra-sonication in acetone, deionized water, and ethanol. The dried substrates were treated with plasma for 15 min and then an OTS self-assembled monolayer was formed by performing OTS treatment on the SiO_2 gate dielectrics in a vacuum. Before the deposition of the polymers, the polymers were dissolved (3 mg mL^{-1}) in the solvent. Before deposition, the solvent was heated and refluxed overnight for complete dissolution of the polymers. Then the semiconductor layer was deposited on the substrates by spin coating at a speed of 2000 rpm for 120 s. For the annealing of FETs, the samples were placed on a hotplate in air for 5 min before cooling down to room temperature. The FET devices tested for PD-*n*-DTTE-7s had a channel length of 50 μm and a channel width of 1400 μm. The evaluation of the polymer FET devices was accomplished using a Keithley 4200 SCS semiconductor parameter analyser on a probe stage.

Results and discussion

Synthesis and theory calculations

The synthetic routes of copolymers PD-*n*-DTTE-7 are shown in Scheme 1. The starting material **1**, synthesized according to the reported literature,[13] was brominated with *N*-bromosuccinimide to give intermediate **2** as a colourless oil. Then intermediate **2** reacted with *n*-BuLi, and quenched with piperidine-

 This journal is © The Royal Society of Chemistry 2016

Published on 20 May 2016. Downloaded by Synchrotron Radiation Library on 11/09/2017 09:39:33.

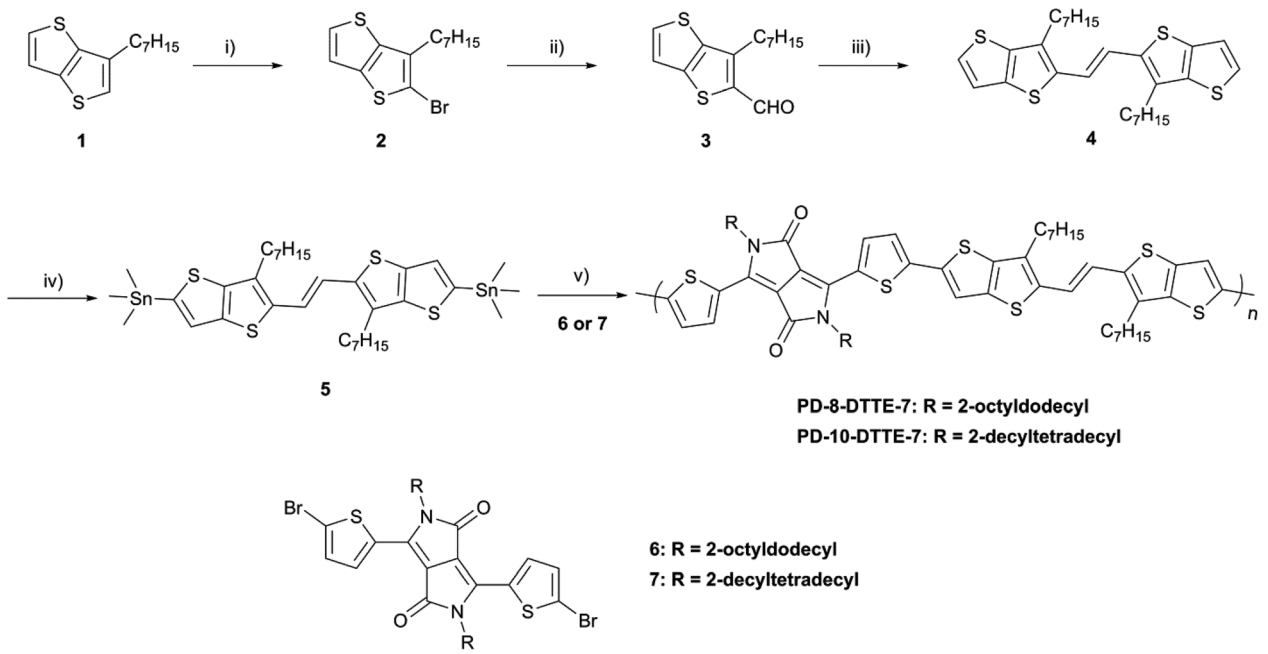

Scheme 1 Reagents and conditions: (i) NBS, $CHCl_3$, 0 °C; (ii) *n*-BuLi, piperidine-1-carboxaldehyde, THF, −78 °C; (iii) Zn, $TiCl_4$, THF, reflux; (iv) *n*-BuLi, Me_3SnCl, THF, −78 °C; (v) $Pd_2(dba)_3$, P(*o*-tol)$_3$, toluene, 110 °C.

1-carboxaldehyde affording aldehyde **3**. In the presence of Zn powder, aldehyde **3** was converted to alkylated-DTTE **4**, by conducting a McMurry reaction. The pure tin monomer **5** was synthesized *via* a conventional method in high yield of 70%. Stille copolymerization of tin monomer **5** and TDPP monomers afforded the crude copolymers. After careful purification by Soxhlet extraction for the removal of low-molecular-weight impurities and a Pd-based catalyst, chlorobenzene was used to extract the target copolymers as a black film-like solid in 67–70% yields. GPC measurements with 1,2,4-trichlorobenzene as the eluent demonstrated the relatively high purity of the high number average molecular weight component (M_n) of 182 kDa for PD-10-DTTE-7 and 74 kDa for PD-8-DTTE-7 with the corresponding PDI of 2.91 and 2.75, respectively (Fig. S1†). The shoulder in the GPC chromatograms may be attributed to the tendency of the polymers to aggregate.[14] All the polymers showed poor solubility in some highly volatile solvents, such as methylene chloride, THF, and chloroform. In halogenated aromatic solvents such as chlorobenzene or 1,2-dichlorobenzene (DCB) with a high boiling point, the two polymers exhibited relatively good solubility (calculated to be 4.22 mg mL^{-1} for PD-8-DTTE-7 and 6.45 mg mL^{-1} for PD-10-DTTE-7 at 80 °C in DCB), which is essential for solution processes. Both high M_n and good solubility act as important variables for obtaining high-performance OFET devices.[6] The thermal behaviour of the polymers was also measured through TGA under a nitrogen atmosphere at a heating rate of 10 °C min^{-1} as shown in Fig. S2.† All the polymers have good thermal stability with decomposition temperatures (5% weight loss) of over 300 °C.

To gain more insight into the structural information of the alkylated-DTTE based copolymers, density functional theory (DFT) calculations of the model compounds, thiophene-flanked DTTE (D1), 6,6′-alkyl chain substituted DTTE (D2), and 3,3′-alkyl chain substituted DTTE (D3), were performed to simulate the polymer backbone (Fig. 1). The side chains were shortened to *n*-propyl groups in order to simplify the calculations, while still maintaining the similar steric bulk effect. Calculation results show that the D1 owns almost a planar structure, where the two torsion angles are 0.2 and 17.3°, respectively. When the *n*-propyl groups are substituted at the 6,6′-positions, the two torsion angles of D2 change to 0.2° and 37.8°, respectively, indicating a serious backbone distortion at the thiophene linkage. For the D3 unit, however, both of its torsion angles are similar to those of the D1 unit, implying a maintained planar structure when chains are introduced into

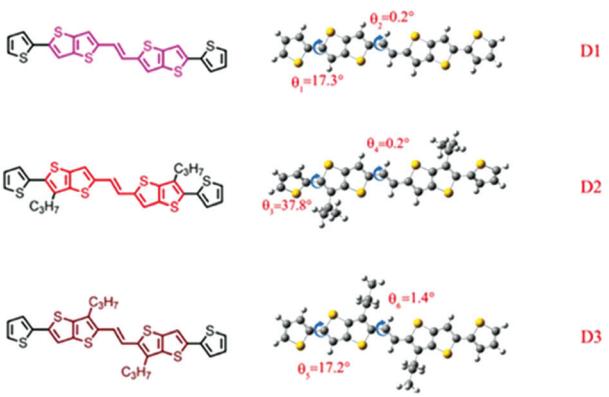

Fig. 1 Energy minimum geometries of the DTTE derivatives with dihedral angles.

Published on 20 May 2016. Downloaded by Synchrotron Radiation Library on 11/09/2017 09:39:33.

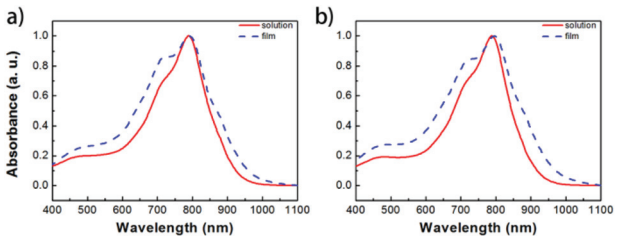

Fig. 2 UV-vis-NIR absorption spectra of (a) PD-8-DTTE-7 and (b) PD-10-DTTE-7 in DCB solution and thin films.

the site adjacent to the vinylene linkage. The calculation results suggest that the attaching position of alkyl side chains has important influence on the coplanarity of alkylated-DTTE and the related copolymers. The torsional disorder along the backbone will limit the effective conjugation length, thus impeding the intrachain transport of charge carriers. Computational analysis of the trimers of copolymers PD-*n*-DTTE-7 shows that the frontier orbital plots are also similar to that of the unalkylated DTTE-polymers (Fig. S3†), indicating that the heptyl groups have negligible influence on the conjugation degree of the polymer backbone.

Optical and electrochemical properties

The UV–vis–NIR absorption spectra of copolymers PD-*n*-DTTE-7 (n = 8 or 10) in solutions and thin films are shown in Fig. 2. PD-*n*-DTTE-7 displays similar absorption spectra to those of unalkylated DTTE-polymers PTDPP-DTTE with the same backbone.[12] Both the polymers PD-*n*-DTTE-7 exhibit broad low-energy bands from 550 to 950 nm due to the strong intramolecular charge transfer (ICT) between the electron-donating units and the electron-withdrawing ones. For PD-*n*-DTTE-7 from solution to film, no significant shift of the absorption spectra was observed, suggesting that some pre-aggregations are formed in solution due to the strong intermolecular interactions of the polymers.[15] An obvious vibronic coupling absorption shoulder at this band was also observed and the intensity of this peak in the film increases compared to that in the respective solution. The HOMO energy levels of PD-8-DTTE-7 (−5.32 eV) and PD-10-DTTE-7 (−5.33 eV) (Fig. S4†) are close to that of unalkylated PTDPP-DTTE.[12] The HOMO energy levels facilitate the hole injections from source–drain Au electrodes, with the work function of 5.1 eV, to polymeric semiconductors, thus is generally beneficial to obtaining high-performance OFET devices. This observation suggests no apparent change in optical properties on attaching extra side chains.

Properties of the field-effect transistors

Bottom-gate bottom-contact (BGBC) FETs were fabricated to investigate field-effect properties of the two polymers. The polymer films were deposited by spin coating a polymer solution of 3 mg mL^{-1} in DCB onto octadecyltrichlorosilane (OTS)-modified Si/SiO_2 (300 nm) substrates. Both the copolymers displayed typical p-type transport characteristics under ambient

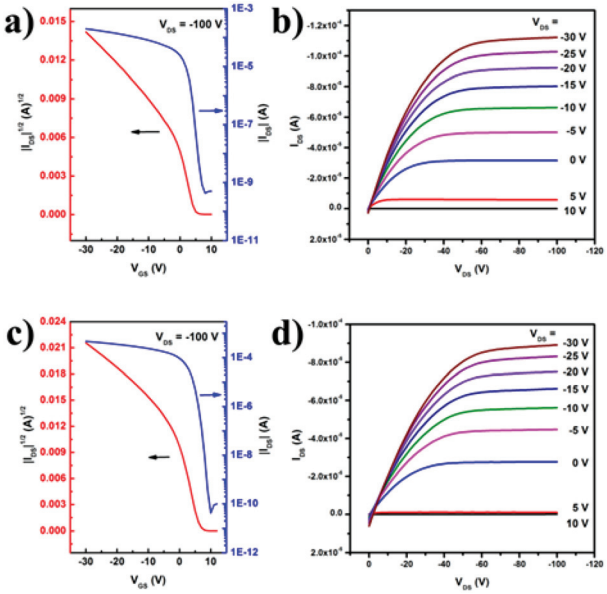

Fig. 3 Transfer (left) and output (right) curves of BGBC FET devices based on PD-8-DTTE-7 (top) and PD-10-DTTE-7 (bottom) thin films. Device dimensions: channel length L = 50 μm; channel width W = 1.4 mm.

conditions. After trying several annealing temperatures, 140 °C was found to give the best device performance for both the polymers (Fig. S5†). Typical transfer and output curves of the FETs are provided in Fig. 3 and the parameters are collected in Table 2. Both the polymers show similar transfer curves to the unalkylated DTTE-polymers PTDPP-DTTE.[16] The maximum mobility reaches 8.49 $cm^2\ V^{-1}\ s^{-1}$ for PD-8-DTTE-7 and 9.54 $cm^2\ V^{-1}\ s^{-1}$ for PD-10-DTTE-7. High average mobilities were calculated to be 5.68 $cm^2\ V^{-1}\ s^{-1}$ for PD-8-DTTE-7 and 8.16 $cm^2\ V^{-1}\ s^{-1}$ for PD-10-DTTE-7. It is worthy of note that the mobility values are much higher than those for the unalkylated DTTE-polymers PTDPP-DTTE.[12] Moreover, polymers of the same backbone with side chains substituted at the thiophene linkage exhibit decreased mobility compared with PTDPP-DTTE,[16] which agree with the calculation result. These values demonstrate the great influence of the substitution positions on the performance of the polymers as FETs, and side chains should be introduced at the position that does not disturb the coplanarity of the backbone. The enhanced mobility compared with the unalkylated DTTE-polymers PTDPP-DTTE may be attributed to the improved solubility of the corresponding polymers by introducing extra soluble side chains. Solubility plays an important role in promoting the electronic performance of polymer seminconductors.[17] The poor solubility of the high molecular weight polymers, often with small gel particles, can disturb the formation of films with high quality and coherence. Improving the solubility of the polymers by introducing side chains could readily prevent too strong aggregation between the polymer chains, thus promoting the formation of more uniform films. Moreover, arising from the improved solubility, high purity of the high

 This journal is © The Royal Society of Chemistry 2016

Published on 20 May 2016. Downloaded by Synchrotron Radiation Library on 11/09/2017 09:39:33.

Table 2 FET properties and relevant crystallographic parameters of the two polymers

Polymer	μ^a ($cm^2\ V^{-1}\ s^{-1}$) Average[b]	Max	I_{on}/I_{off}	V_{th} (V)	π–π spacing[c] (Å)	Lamellar spacing[b] (Å)
PD-8-DTTE-7	5.68	8.49	10^6–10^7	2.65–5.74	3.84	19.08
PD-10-DTTE-7	8.16	9.54	10^5–10^7	3.37–6.08	3.85	20.10

[a] The mobilities were calculated in the linear range of 0–5 V. [b] The values were calculated from 10 devices. [c] The stacking distances were calculated from the annealed films.

molecular weight component is achieved by extraction (Fig. S1†), which is one of the factors for obtaining high performance.[6] In some cases, solubility even plays a more important role than the structure of the polymers does.[1d]

Thin film microstructural characterization

In order to investigate the morphology and crystallinity of the films, thin films of the polymers were characterized by atomic force microscopy (AFM) and 2D grazing-incidence X-ray diffraction (GIXRD). AFM topographies and two-dimensional GIXRD images of the annealed thin films for both the polymers are illustrated in Fig. 4, and the corresponding parameters are collected in Table 2. The AFM topographies display two coherent films with no significant grain boundaries, indicating the high uniformity of the films. In the out-of-plane pattern of the GIXRD images, the thermally annealed films of both the polymers show clear diffraction peaks of (100), (200), (300), and additional diffraction peaks of (400), corresponding to the *d*-spacing of 19.35 Å for PD-8-DTTE-7 and 20.55 Å for PD-10-DTTE-7. Another (010) peak appears in the in-plane pattern. The GIXRD results revealed the formation of a highly ordered layer-by-layer lamellar packing motif with an edge-on orientation for the thin films. On the basis of the aforementioned results, the polymers show an aggregation tendency with ordered packing, which would benefit interchain transport. Compared with the other similar systems of PTDPP-DTTE[12] and PDTTE,[16] the (010) peaks are much weaker, indicating less crystallinity of the PD-*n*-DTTE-7s. Although PDTTE exhibits better crystallinity, the distortion of the backbone still limits the intrachain transport, indicating the importance of charge transport along the polymer backbone.

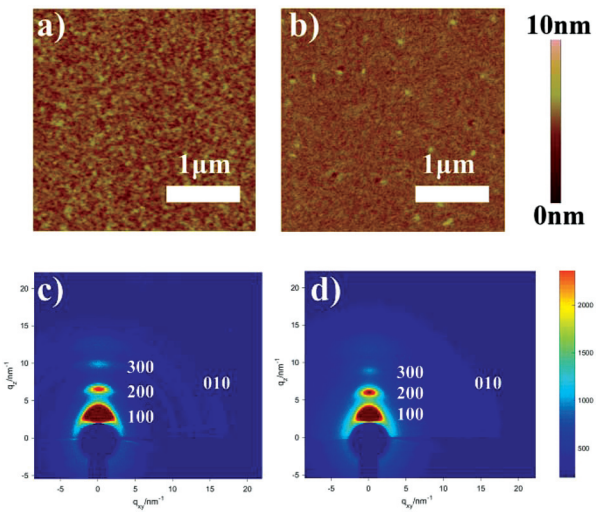

Fig. 4 AFM height images (3 × 3 μm) and GIXRD detector images of thin films of PD-8-DTTE-7 (a and c) and PD-10-DTTE-7 (b and d) annealed at 140 °C in air for 5 min.

For both the D–A alkylated polymers with the small alkylated units such as 3,3′-alkylated-2,2′-bithiophene or (*E*)-1,2-bis-(3-alkylated-thiophen-2-yl)ethene, no evidence of π–π stacking were observed.[9d,18] This can be attributed to the too crowded side chain density, which hinders the molecule stacking. However, obvious stacking can be detected in the alkylated-DTTE based polymers of PDTTE[16] and PD-*n*-DTTE-7, although the intensity is somewhat weak. These results suggest the existence of ordered stacking in the solid state of the alkylated-DTTE based polymers. The possible stacking structures are shown in Fig. 5. The large space between the clusters of the alkyl chains of PDTTE will facilitate interdigitation of side chains, thus favouring the formation of lamellar packing structures.[19] Although the space of PD-*n*-DTTE-7s was not that large, it could also guarantee the interdigitations and stacking in films. This could also explain the less crystallinity of the PD-*n*-DTTE-7s while maintaining a similar π–π stacking distance to PDTTE.[16] When the polymers stack together, direct overlap for D–A or A–A units exhibits higher energy because of the strong repulsion between the alkyl chains.[9e] The polymers may adopt a "slide" configuration with the neighbouring polymers (Fig. 5d and e). The space between the branched chains is divided by the linear alkyl chains into which another polymer chain "docks", leading to a direct interchain interaction between DPP and thienothiophene moieties. Note that the π–π distances for PD-*n*-DTTE-7 are much higher than that for the unalkylated DTTE-polymer PTDPP-DTTE, which was generally thought to be unfavourable for intermolecular charge hopping.[20] The longer stacking distance may be attributed to the slightly blocked interdigitation (Fig. 5e). The interchain charge transport is affected by the π–π interactions of the polymers, but the interchain stacking distances should not be overemphasized. In fact, low mobility can be obtained with a short π–π stacking distance,[3e] and long distances also lead to high performance.[21] Recent studies also revealed that the longer π–π stacking distance did afford better performance, and the paracrystalline nature and (*h*00) plane distribution played a

Published on 20 May 2016. Downloaded by Synchrotron Radiation Library on 11/09/2017 09:39:33.

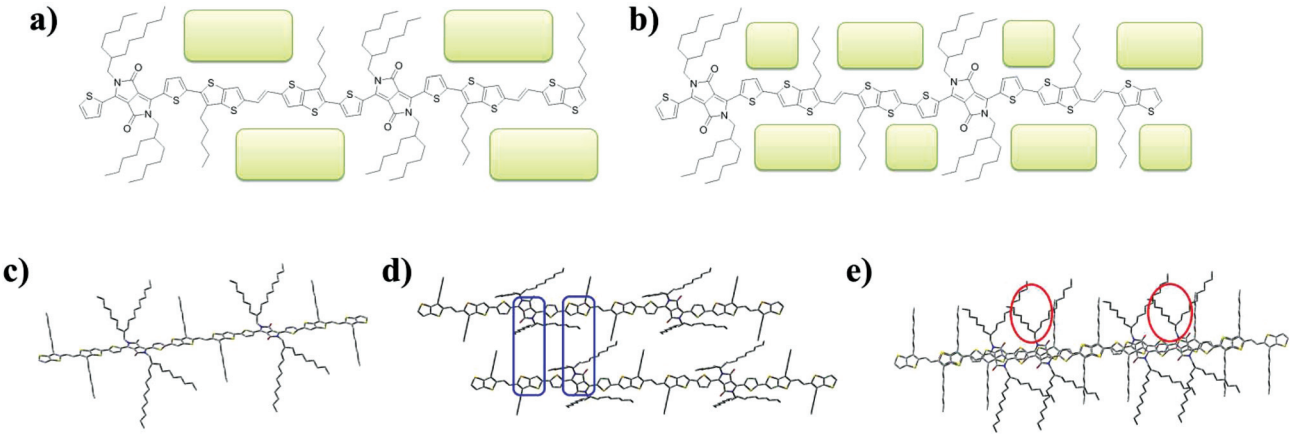

Fig. 5 Illustrated structures of the alkylated-DTTE based polymers. The chemical structures of (a) PDTTE and (b) PD-*n*-DTTE-7s; (c) simplified structures of the PD-*n*-DTTE-7s; illustrated structures in the direction perpendicular to the polymer backbone in side view (d) and front view (e).

critical role.[21b] Moreover, Zhao *et al.* also demonstrated the crucial role of the intrachain transport in polymer based FETs.[22] For these, the intrachain transport may have advantages over interchain transport and the stacking distance may not be the primary reason in improving mobilities.

Conclusions

In conclusion, two highly soluble alternating copolymers with donors and acceptors alkylated were strategically synthesized and characterized. The improved solubility arising from the increased side chain density leads to high purity of high molecular weight polymers and uniform thin films. In addition, by carefully selecting the large donor moieties of DTTE and the side chain substitution position adjacent to the vinyl linkage, ordered packing and backbone coplanarity are maintained, which are beneficial for interchain and intrachain charge transport. Both the polymers show high average hole mobility over 5 $cm^2 V^{-1} s^{-1}$, through a simple spin coating method, and the highest value reached 9.54 $cm^2 V^{-1} s^{-1}$ for PD-8-DTTE-7, which are among the highest for polymer-based FETs. The mobility of PD-*n*-DTTE-7 with both the donor and acceptor alkylated was higher compared to the polymers alkylated on one moiety. This substitution strategy is valuable for further design of highly soluble polymer semiconductors with a high molecular weight.

Acknowledgements

This work was financially supported by the Strategic Priority Research Program of the Chinese Academy of Sciences (XDB12030100) and the National Natural Science Foundation of China (21474116 and 51233006). The GIXRD results were tested at 23A1 Station (National Synchrotron Radiation Research Center, Taiwan), BL14B1 (Shanghai Synchrotron Radiation Facility), and 1W1A (Beijing Synchrotron Radiation Facility). The authors gratefully appreciate the assistance of scientists from the stations during the experiments.

Notes and references

1 (*a*) W. Wu, Y. Liu and D. Zhu, *Chem. Soc. Rev.*, 2010, **39**, 1489; (*b*) H. Chen, Y. Guo, G. Yu, Y. Zhao, J. Zhang, D. Gao, H. Liu and Y. Liu, *Adv. Mater.*, 2012, **24**, 4618; I. Kang, T. K. An, J. A. Hong, H. J. Yun, R. Kim, D. S. Chung, C. E. Park, Y. H. Kim and S. K. Kwon, *Adv. Mater.*, 2013, **25**, 524; (*c*) X. G. Guo, A. Facchetti and T. J. Marks, *Chem. Rev.*, 2014, **114**, 8943; (*d*) M. Al-Hashimi, Y. Han, J. Smith, H. S. Bazzi, S. Y. A. Alqaradawi, S. E. Watkins, T. D. Anthopoulos and M. Heeney, *Chem. Sci.*, 2016, **7**, 1093; (*e*) M. Wang, M. Ford, H. Phan, J. Coughlin, T.-Q. Nguyenabcd and G. C. Bazan, *Chem. Commun.*, 2016, **52**, 3207; (*f*) W. Zhang, N. Zheng, C. Wei, J. Huang, D. Gao, K. Shi, J. Xu, D. Yan, Y. Han and G. Yu, *Polym. Chem.*, 2016, **7**, 1413.

2 (*a*) J. Li, Y. Zhao, H. S. Tan, Y. L. Guo, C. A. Di, G. Yu, Y. Q. Liu, M. Lin, S. H. Lim, Y. Zhou, H. Su and B. S. Ong, *Sci. Rep.*, 2012, **2**, 754; (*b*) I. Kang, H. J. Yun, D. S. Chung, S. K. Kwon and Y. H. Kim, *J. Am. Chem. Soc.*, 2013, **135**, 14896; (*c*) H. R. Tseng, H. Phan, C. Luo, M. Wang, L. A. Perez, S. N. Patel, L. Ying, E. J. Kramer, T. Q. Nguyen, G. C. Bazan and A. J. Heeger, *Adv. Mater.*, 2014, **26**, 2993; (*d*) G. Kim, S.-J. Kang, G. K. Dutta, Y.-K. Han, T. J. Shin, Y.-Y. Noh and C. Yang, *J. Am. Chem. Soc.*, 2014, **136**, 9477; (*e*) J. Y. Back, H. Yu, I. Song, I. Kang, H. Ahn, T. J. Shin, S.-K. Kwon, J. H. Oh and Y.-H. Kim, *Chem. Mater.*, 2015, **27**, 1732; (*f*) Y. Ji, C. Xiao, Q. Wang, J. Zhang, C. Li, Y. Wu, Z. Wei, X. Zhan, W. Hu, Z. Wang, R. A. J. Janssen and W. Li, *Adv. Mater.*, 2016, **28**, 943; (*g*) J. Yao, C. Yu, Z. Liu, H. Luo, Y. Yang, G. Zhang and D. Zhang, *J. Am. Chem. Soc.*, 2016, **138**, 173.

3 (*a*) Z. Chen, M. J. Lee, R. S. Ashraf, Y. Gu, S. Albert-Seifried, M. M. Nielsen, B. Schroeder, T. D. Anthopoulos,

 This journal is © The Royal Society of Chemistry 2016

Published on 20 May 2016. Downloaded by Synchrotron Radiation Library on 11/09/2017 09:39:33.

M. Heeney, L. McCulloch and H. Sirringhaus, *Adv. Mater.*, 2012, **24**, 647; (*b*) J. S. Lee, S. K. Son, S. Song, H. Kim, D. R. Lee, K. Kim, M. J. Ko, D. H. Choi, B. S. Kim and J. H. Cho, *Chem. Mater.*, 2012, **24**, 1316; (*c*) M. Kaur, D. S. Yang, J. Shin, T. W. Lee, K. Choi, M. J. Cho and D. H. Choi, *Chem. Commun.*, 2013, **49**, 5495; (*d*) M. Gruber, S.-H. Jung, S. Schott, D. Venkateshvaran, A. J. Kronemeijer, J. W. Andreasen, C. R. McNeill, W. W. H. Wong, M. Shahid, M. Heeney, J.-K. Lee and H. Sirringhaus, *Chem. Sci.*, 2015, **6**, 6949; (*e*) A. Keerthi, C. An, M. Li, T. Marszalek, A. G. Ricciardulli, B. Radha, F. D. Alsewailem, K. Müllen and M. Baumgarten, *Polym. Chem.*, 2016, **7**, 1545.

4 (*a*) T. Lei, J. Y. Wang and J. Pei, *Chem. Mater.*, 2014, **26**, 594; (*b*) C. Guo, J. Quinn, B. Sun and Y. Li, *J. Mater. Chem. C*, 2015, **3**, 5226; (*c*) Z. Yi, L. Ma, P. Li, L. Xu, X. Zhan, J. Qin, X. Chen, Y. Liu and S. Wang, *Polym. Chem.*, 2015, **6**, 5369; (*d*) Y. He, C. Guo, B. Sun, J. Quinn and Y. Li, *Polym. Chem.*, 2015, **6**, 6689.

5 (*a*) X. Zhang, L. J. Richter, D. M. DeLongchamp, R. J. Kline, M. R. Hammond, I. McCulloch, M. Heeney, R. S. Ashraf, J. N. Smith, T. D. Anthopoulos, B. Schroeder, Y. H. Geerts, D. A. Fischer and M. F. Toney, *J. Am. Chem. Soc.*, 2011, **133**, 15073; (*b*) C. Cabanetos, A. E. Labban, J. A. Bartelt, J. D. Douglas, W. R. Mateker, J. J. Fréchet, M. D. McGehee and P. M. Beaujuge, *J. Am. Chem. Soc.*, 2013, **135**, 4656; (*c*) H. S. Marsh, E. Jankowski and A. Jayaraman, *Macromolecules*, 2014, **47**, 2736; (*d*) Z.-H. Guo, N. Ai, C. R. McBroom, T. Yuan, Y.-H. Lin, M. Roders, C. Zhu, A. L. Ayzner, J. Pei and L. Fang, *Polym. Chem.*, 2016, **7**, 648.

6 (*a*) A. Zen, J. Pflaum, S. Hirschmann, W. Zhuang, F. Jaiser, U. Asawapirom, J. P. Rabe, U. Scherf and D. Neher, *Adv. Funct. Mater.*, 2004, **14**, 8; (*b*) R. J. Kline, M. D. McGehee, E. N. Kadnikova, J. Liu, J. M. J. Fréchet and M. F. Toney, *Macromolecules*, 2005, **38**, 3312; (*c*) L. H. Jimison, M. F. Toney, I. McCulloch, M. Heeney and A. Salleo, *Adv. Mater.*, 2009, **21**, 1568; (*d*) M. Tong, S. Cho, J. T. Rogers, K. Schmidt, B. B. Y. Hsu, D. Moses, R. C. Coffin, E. J. Kramer, G. C. Bazan and A. J. Heeger, *Adv. Funct. Mater.*, 2010, **20**, 3959; (*e*) H. N. Tsao, D. M. Cho, I. Park, M. R. Hansen, A. Mavrinskiy, D. Y. Yoon, R. Graf, W. Pisula, H. W. Spiess and K. Müllen, *J. Am. Chem. Soc.*, 2011, **133**, 2605.

7 I. McCulloch, R. S. Ashraf, L. Biniek, H. Bronstein, C. Combe, J. E. Donaghey, D. I. James, C. B. Nielsen, B. C. Schroeder and W. Zhang, *Acc. Chem. Res.*, 2012, **45**, 714.

8 (*a*) J. Kim, B. Lim, K.-J. Baeg, Y.-Y. Noh, D. Khim, H.-G. Jeong, J.-M. Yun and D.-Y. Kim, *Chem. Mater.*, 2011, **23**, 4663; (*b*) I. Osaka, T. Kakara, N. Takemura, T. Koganezawa and K. Takimiya, *J. Am. Chem. Soc.*, 2013, **135**, 8834; (*c*) H. S. Marsh, O. G. Reid, G. Barnes, M. Heeney, N. Stingelin and G. Rumbles, *J. Polym. Sci., Part B: Polym. Phys.*, 2014, **52**, 700; (*d*) K.-Y. Wu, C.-C. Chiu, W.-T. Chuang, C.-L. Wang and C.-S. Hsu, *Polym. Chem.*, 2015, **6**, 1309; (*e*) P. Liu, S. Dong, F. Liu, X. Hu, L. Liu, Y. Jin, S. Liu, X. Gong, T. P. Russell, F. Huang and Y. Cao, *Adv. Funct. Mater.*, 2015, **25**, 6458.

9 (*a*) L. Burgi, M. Turbiez, R. Pfeiffer, F. Bienewald, H. J. Kirner and C. Winnewisser, *Adv. Mater.*, 2008, **20**, 2217; (*b*) Y. Li, P. Sonar, S. P. Singh, M. S. Soh, M. van Meurs and J. Tan, *J. Am. Chem. Soc.*, 2011, **133**, 2198; (*c*) J. C. Bijleveld, R. A. M. Verstrijden, M. M. Wienk and R. J. Janssen, *J. Mater. Chem.*, 2011, **21**, 9224; (*d*) X. Guo, F. S. Kim, M. J. Seger, S. A. Jenekhe and M. D. Watson, *Chem. Mater.*, 2012, **24**, 1434; (*e*) T. Lei, Y. Cao, X. Zhou, Y. Peng, J. Bian and J. Pei, *Chem. Mater.*, 2012, **24**, 1762.

10 (*a*) Y. Li, P. Sonar, S. P. Singh, Z. E. Ooi, E. S. H. Lek and M. Q. Y. Loh, *Phys. Chem. Chem. Phys.*, 2012, **14**, 7162; (*b*) M. J. Cho, J. Shin, S. H. Yoon, T. W. Lee, M. Kaur and D. H. Choi, *Chem. Commun.*, 2013, **49**, 7132; (*c*) S. Park, B. T. Lim, B. S. Kim, H. J. Son and D. S. Chung, *Sci. Rep.*, 2014, **4**, 5482.

11 K. Takimiya, S. Shinamura, I. Osaka and E. Miyazaki, *Adv. Mater.*, 2011, **23**, 4347.

12 J. Shin, T. R. Hong, T. W. Lee, A. Kim, Y. H. Kim, M. J. Cho and D. H. Choi, *Adv. Mater.*, 2014, **26**, 6031.

13 X. Zhang, M. Kohler and A. J. Matzger, *Macromolecules*, 2004, **37**, 6306.

14 J. C. Bijleveld, V. S. Gevaerts, D. D. Nuzzo, M. Turbiez, S. G. J. Mathijssen, D. M. Leeuw, M. M. Wienk and R. A. J. Janssen, *Adv. Mater.*, 2010, **22**, E242.

15 (*a*) J. Kim and T. Swager, *Nature*, 2001, **411**, 1030; (*b*) N. Zhou, X. Guo, R. P. Ortiz, S. Li, S. Zhang, R. P. H. Chang, A. Facchetti and T. J. Marks, *Adv. Mater.*, 2012, **24**, 2242; (*c*) T. Lei, J.-H. Dou, X.-Y. Cao, J.-Y. Wang and J. Pei, *J. Am. Chem. Soc.*, 2013, **135**, 12168; (*d*) J. Kim, A.-R. Han, J. Hong, G. Kim, J. Lee, T. J. Shin, J. H. Oh and C. Yang, *Chem. Mater.*, 2014, **26**, 4933; (*e*) G. Zhang, J. Guo, M. Zhu, P. Li, H. Lu, K. Chod and L. Qiu, *Polym. Chem.*, 2015, **6**, 2531.

16 M. Jang, J.-H. Kim, D.-H. Hwang and H. Yang, *ACS Appl. Mater. Interfaces*, 2015, **7**, 12781.

17 (*a*) L. Fang, Y. Zhou, Y.-X. Yao, Y. Diao, W.-Y. Lee, A. L. Appleton, R. Allen, J. Reinspach, S. C. B. Mannsfeld and Z. Bao, *Chem. Mater.*, 2013, **25**, 4874; (*b*) C. B. Nielsen, R. S. Ashraf, S. Rossbauer, T. Anthopoulos and I. McCulloch, *Macromolecules*, 2013, **46**, 7727; (*c*) B. Fu, J. Baltazar, A. R. Sankar, P.-H. Chu, S. Zhang, D. M. Collard and E. Reichmanis, *Adv. Funct. Mater.*, 2014, **24**, 3734.

18 Z. Cai, Z. Liu, H. Luo, P. Qi, G. Zhang and D. Zhang, *Chin. J. Chem.*, 2014, **32**, 788.

19 Q. Wu, M. Wang, X. Qiao, Y. Xiong, Y. Huang, X. Gao and H. Li, *Macromolecules*, 2013, **46**, 3887.

20 I. McCulloch, M. Heeney, C. Bailey, K. Genevicius, I. MacDonald, M. Shkunov, D. Sparrowe, S. Tierney, R. Wagner, W. Zhang, M. L. Chabinyc, R. J. Kline, M. D. McGehee and M. F. Toney, *Nat. Mater.*, 2006, **5**, 328.

21 (*a*) M. Kaur, D. S. Yang, J. Shin, T. W. Lee, K. Choi, M. J. Cho and D. H. Choi, *Chem. Commun.*, 2013, **49**, 5495; (*b*) D. Yoo, B. Nketia-Yawson, S.-J. Kang, H. Ahn, T. J. Shin, Y.-Y. Noh and C. Yang, *Adv. Funct. Mater.*, 2015, **25**, 586.

22 Y. Zhao, X. Zhao, M. Roders, G. Qu, Y. Diao, A. L. Ayzner and J. Mei, *Chem. Mater.*, 2015, **27**, 7164.